

## Mesoporous Silica Nanoparticles for Intracellular Delivery of Membrane-Impermeable Proteins

Igor I. Slowing, Brian G. Trewyn, and Victor S.-Y. Lin\*

Contribution from the Department of Chemistry, U.S. DOE Ames Laboratory,  
Iowa State University, Ames, Iowa 50011-3111

Received March 20, 2007; E-mail: vsyin@iastate.edu

**Abstract:** An MCM-41-type mesoporous silica nanoparticle (MSN) material with a large average pore diameter (5.4 nm) is synthesized and characterized. The in vitro uptake and release profiles of cytochrome *c* by the MSN were investigated. The enzymatic activity of the released protein was quantitatively analyzed and compared with that of the native cytochrome *c* in physiological buffer solutions. We found that the enzymes released from the MSNs are still functional and highly active in catalyzing the oxidation of 2,2'-azino-bis(3-ethylbenzthiazoline-6-sulfonate) (ABTS) by hydrogen peroxide. In contrast to the fact that cytochrome *c* is a cell-membrane-impermeable protein, we discovered that the cytochrome *c*-encapsulated MSNs could be internalized by live human cervical cancer cells (HeLa) and the protein could be released into the cytoplasm. We envision that these MSNs with large pores could serve as a transmembrane delivery vehicle for controlled release of membrane-impermeable proteins in live cells, which may lead to many important biotechnological applications including therapeutics and metabolic manipulation of cells.

### Introduction

Recent breakthroughs in the synthesis of mesoporous silica materials with high surface areas ( $>800 \text{ m}^2/\text{g}$ ) and tunable pore diameter (2–10 nm) have led to the development of a series of new delivery systems, where various guest molecules, such as pharmaceutical drugs, fluorescent imaging agents, and other molecules, could be adsorbed into the mesopores and later released into various solutions.<sup>1–4</sup> Furthermore, recent reports on the design of functional mesoporous silica materials by decorating the pore surface with organic or inorganic moieties that could serve as gating devices to regulate the release of guest molecules under the control of several different external stimuli, such as chemicals,<sup>5–9</sup> temperature,<sup>10</sup> redox reactions,<sup>11,12</sup> and

photoirradiation,<sup>13,14</sup> have highlighted the potential of utilizing this kind of nanodevice for many controlled release applications.

To further advance this burgeoning field of research and to use these mesoporous materials in practical biotechnological and biomedical applications, one key step would be to gain control of the particle morphology and the surface properties of these inorganic oxides so that the compatibility with biological macromolecules, such as polynucleotides (DNA and RNA), proteins, and live cells, can be enhanced. We and others have demonstrated that, by controlling the particle size, shape, and surface functionality of the mesoporous silicas, these structurally defined materials can be efficiently endocytosed by live cells with high biocompatibility in vitro and serve as delivery vehicles for the controlled release of genes and membrane-impermeable chemicals.<sup>3,5–7</sup>

Also, several enzymes have been shown to be functional without being denatured inside the frameworks of mesoporous silicas, such as MCM-41 and SBA-15 silicas.<sup>15–23</sup> However, to the best of our knowledge, there were only two prior reports

- (1) Gruenhagen, J. A.; Lai, C.-Y.; Radu, D. R.; Lin, V. S. Y.; Yeung, E. S. *Appl. Spectrosc.* **2005**, *59*, 424–431.
- (2) Horcajada, P.; Ramila, A.; Perez-Pariente, J.; Vallet-Regi, M. *Microporous Mesoporous Mater.* **2004**, *68*, 105–109.
- (3) Trewyn, B. G.; Whitman, C. M.; Lin, V. S. Y. *Nano Lett.* **2004**, *4*, 2139–2143.
- (4) Balas, F.; Manzano, M.; Horcajada, P.; Vallet-Regi, M. *J. Am. Chem. Soc.* **2006**, *128*, 8116–8117.
- (5) Giri, S.; Trewyn, B. G.; Stellmaker, M. P.; Lin, V. S. Y. *Angew. Chem., Int. Ed.* **2005**, *44*, 5038–5044.
- (6) Lai, C.-Y.; Trewyn, B. G.; Jeftinija, D. M.; Jeftinija, K.; Xu, S.; Jeftinija, S.; Lin, V. S. Y. *J. Am. Chem. Soc.* **2003**, *125*, 4451–4459.
- (7) Radu, D. R.; Lai, C.-Y.; Jeftinija, K.; Rowe, E. W.; Jeftinija, S.; Lin, V. S. Y. *J. Am. Chem. Soc.* **2004**, *126*, 13216–13217.
- (8) Leung, K. C. F.; Nguyen, T. D.; Stoddart, J. F.; Zink, J. I. *Chem. Mater.* **2006**, *18*, 5919–5928.
- (9) Nguyen, T. D.; Leung, K. C. F.; Liong, M.; Pentecost, C. D.; Stoddart, J. F.; Zink, J. I. *Org. Lett.* **2006**, *8*, 3363–3366.
- (10) Fu, Q.; Rao, G. V. R.; Ista, L. K.; Wu, Y.; Andrzejewski, B. P.; Sklar, L. A.; Ward, T. L.; Lopez, G. P. *Adv. Mater. (Weinheim, Ger.)* **2003**, *15*, 1262–1266.
- (11) Hernandez, R.; Tseng, H.-R.; Wong, J. W.; Stoddart, J. F.; Zink, J. I. *J. Am. Chem. Soc.* **2004**, *126*, 3370–3371.
- (12) Nguyen, T. D.; Tseng, H.-R.; Celestre, P. C.; Flood, A. H.; Liu, Y.; Stoddart, J. F.; Zink, J. I. *Proc. Natl. Acad. Sci. U.S.A.* **2005**, *102*, 10029–10034.

- (13) Mal, N. K.; Fujiwara, M.; Tanaka, Y. *Nature (London)* **2003**, *421*, 350–353.
- (14) Mal, N. K.; Fujiwara, M.; Tanaka, Y.; Taguchi, T.; Matsukata, M. *Chem. Mater.* **2003**, *15*, 3385–3394.
- (15) Deere, J.; Magner, E.; Wall, J. G.; Hodnett, B. K. *J. Phys. Chem. B* **2002**, *106*, 7340–7347.
- (16) Diaz, J. F.; Balkus, K. J., Jr. *J. Mol. Catal. B: Enzym.* **1996**, *2*, 115–126.
- (17) Hartmann, M. *Chem. Mater.* **2005**, *17*, 4577–4593.
- (18) Vinu, A.; Murugesan, V.; Tangermann, O.; Hartmann, M. *Chem. Mater.* **2004**, *16*, 3056–3065.
- (19) Lee, C.-H.; Mou, C.-Y.; Ke, S.-C.; Lin, T.-S. *Mol. Phys.* **2006**, *104*, 1635–1641.
- (20) Cheng, Y. Y.; Lin, S. H.; Chang, H. C.; Su, M. C. *J. Phys. Chem. A* **2003**, *107*, 10687–10694.
- (21) Katiyar, A.; Ji, L.; Smirniotis, P.; Pinto, N. G. *J. Chromatogr., A* **2005**, *1069*, 119–126.
- (22) Lei, J.; Fan, J.; Yu, C.; Zhang, L.; Jiang, S.; Tu, B.; Zhao, D. *Microporous Mesoporous Mater.* **2004**, *73*, 121–128.
- (23) Yiu, H. H. P.; Wright, P. A. *J. Mater. Chem.* **2005**, *15*, 3690–3700.

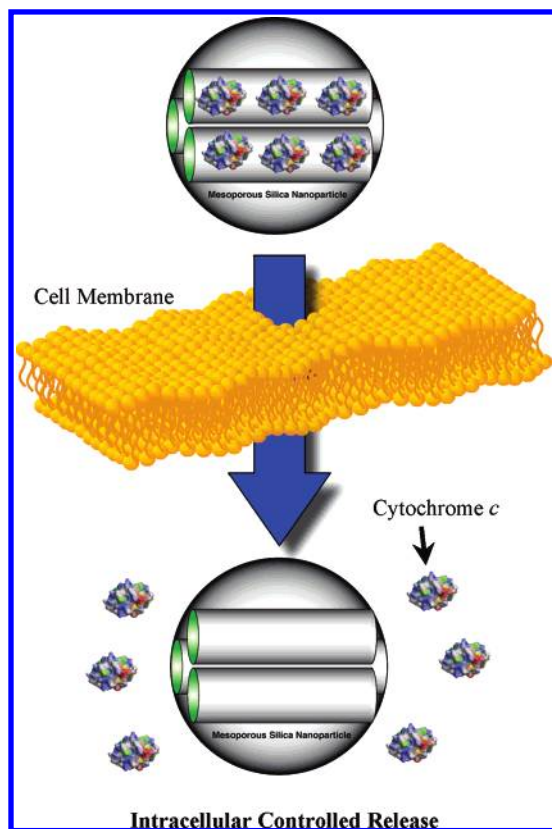


**Figure 1.** Schematic representation of the MSN transporting cytochrome *c* through the cell membrane and releasing the protein into the cytoplasm.

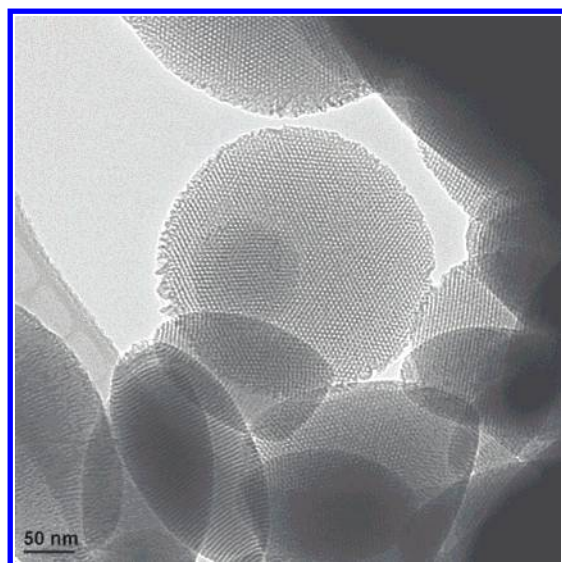


**Figure 2.** Transmission electron micrograph of large-pore MSN.

on the controlled release of proteins from SBA-15-type mesoporous silica materials under nonphysiological conditions.<sup>24,25</sup> Since the intracellular delivery of membrane-impermeable proteins is an important research topic for understanding metabolic pathways of different cell types as well as for therapeutic applications, different cell-penetrating molecular agents and materials, such as peptides,<sup>26,27</sup> polymers,<sup>28</sup> and

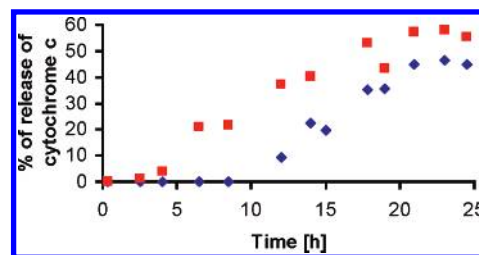


**Figure 3.** Release profiles of cytochrome *c* from MSN at pH 7.4 (blue rhombi) and 5.2 (red squares).

carbon nanotubes,<sup>29–31</sup> have been employed as carriers for this purpose with different degrees of success. For example, single-wall carbon nanotubes have been demonstrated recently to be able to deliver a cell-membrane-impermeable protein, cytochrome *c*, into cells. However, the protein–nanotube composites were unable to escape endosomal entrapment without the introduction of an endosome-disrupting agent, chloroquine, to the cells.<sup>29</sup> In contrast to these prior systems, there are several advantages of using mesoporous silicas for intracellular protein delivery: (1) The large pore volumes ( $> 1 \text{ cm}^3/\text{g}$ ) of mesoporous silicas allow for loading vast, yet quantifiable, amounts of proteins into the particles. (2) The chemically and mechanically stable inorganic oxide framework of mesoporous silicas shelters the protein molecules from exposure to harmful species, such as proteases and denaturation chemicals. (3) It has been previously observed that mesoporous silica nanoparticles (MSNs) are able to escape the endolysosomal entrapment.<sup>32–34</sup> Therefore, the particles could serve not only as vehicles for introducing the proteins into the cells but also to enable their release into the cytoplasm.

Herein, we report on the synthesis and characterization of an MCM-41-type MSN material with a large pore diameter (5.4 nm). The uptake and release profiles of cytochrome *c* by the MSN were investigated. To examine whether the encapsulation causes any harmful effect to cytochrome *c*, we analyzed the enzymatic activity of the pore-released protein and compared with that of the native cytochrome *c* in physiological buffer solutions. In addition, we discovered that the cytochrome *c*-encapsulated MSNs could be internalized by living human cervical cancer cells (HeLa) and the protein could be released into the cytoplasm as depicted in Figure 1.

## Results and Discussion

As detailed in the Supporting Information, we synthesized MSN with large pores by adding a pore-expanding agent (mesitylene) to a CTAB-templated, base-catalyzed condensation reaction of silicate that we have previously reported.<sup>35</sup> The template-removed MSN material is comprised of an MCM-41-

(24) Han, Y.-J.; Stucky, G. D.; Butler, A. *J. Am. Chem. Soc.* **1999**, *121*, 9897–9898.

(25) Song, S. W.; Hidajat, K.; Kawi, S. *Langmuir* **2005**, *21*, 9568–9575.

(26) Ye, D.; Xu, D.; Singer, A. U.; Juliano, R. L. *Pharm. Res.* **2002**, *19*, 1302–1309.

(27) Gros, E.; Deshayes, S.; Morris, M. C.; Aldrian-Herrada, G.; Depollier, J.; Heitz, F.; Divita, G. *Biochim. Biophys. Acta* **2006**, *1758*, 384–393.

(28) Vicent, M. J.; Duncan, R. *Trends Biotechnol.* **2006**, *24*, 39–47.

(29) Kam, N. W. S.; Dai, H. *J. Am. Chem. Soc.* **2005**, *127*, 6021–6026.

(30) Kam, N. W. S.; Jessop, T. C.; Wender, P. A.; Dai, H. *J. Am. Chem. Soc.* **2004**, *126*, 6850–6851.

(31) Kam, N. W. S.; Liu, Z.; Dai, H. *Angew. Chem., Int. Ed.* **2006**, *45*, 577–581.

(32) Lin, Y.-S.; Tsai, C.-P.; Huang, H.-Y.; Kuo, C.-T.; Hung, Y.; Huang, D.-M.; Chen, Y.-C.; Mou, C.-Y. *Chem. Mater.* **2005**, *17*, 4570–4573.

(33) Huang, D.-M.; Hung, Y.; Ko, B.-S.; Hsu, S.-C.; Chen, W.-H.; Chien, C.-L.; Tsai, C.-P.; Kuo, C.-T.; Kang, J.-C.; Yang, C.-S.; Mou, C.-Y.; Chen, Y.-C. *FASEB J.* **2005**, *19*, 2014–2016.

(34) Slowing, I.; Trewyn, B. G.; Lin, V. S. Y. *J. Am. Chem. Soc.* **2006**, *128*, 14792–14793.

(35) Huh, S.; Wiensch, J. W.; Yoo, J.-C.; Pruski, M.; Lin, V. S. Y. *Chem. Mater.* **2003**, *15*, 4247–4256.

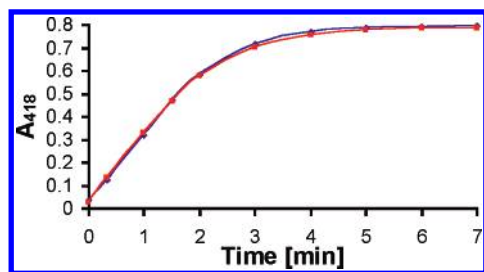


**Figure 4.** Oxidation of 2,2'-azino-bis(3-ethylbenzthiazoline-6-sulfonate) (ABTS) catalyzed by cytochrome *c*. The blue line and markers correspond to a solution of native protein and the red ones to the protein released from the MSN.

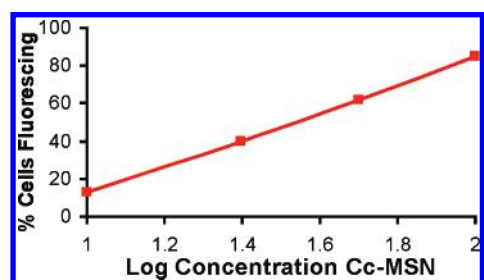


**Figure 5.** Uptake profile of FITC-cytochrome *c*-loaded MSN by HeLa cancer cells.

type, hexagonal array of mesoporous channels as shown in the transmission electron micrographs (TEM) (Figure 2 and Supporting Information Figure SI 1). The powder X-ray diffraction pattern (XRD) further confirmed the hexagonal mesoporous structure (Supporting Information Figure SI 2a) with the  $d_{100}$  value of 71.8 Å,  $d_{110}$  of 40.8 Å,  $d_{200}$  of 35.1 Å, and  $d_{210}$  of 26.2 Å. The nitrogen surface sorption analysis of the material exhibited a type IV isotherm with a BET surface area of 1061 m<sup>2</sup>/g and a pore volume of 1.82 cm<sup>3</sup>/g (Supporting Information Figure SI 2b). The BJH method gave two pore size distributions centered on 5.4 nm (major peak) and 14.5 nm (minor) (Supporting Information Figure SI 2c). Of both pore distributions, the wider ones (>10 nm) appear to correspond to incomplete wall formation in the outermost layer of some particles, as observed by TEM imaging (Figures 2b and Supporting Information SI 1). Thus, the wider pores seem to be entrances shared by two or more of the smaller channel-type pores that run along the particles. The particle size of MSN in PBS suspension was measured by dynamic light scattering. Two different particle size distributions (265 and 933 nm) were observed (Supporting Information Figure SI 3). These particles are spherical and oval-shaped as shown in Figure 2.

We found that the loading of cytochrome *c* (molecular dimensions  $2.6 \times 3.2 \times 3.3$  nm<sup>3</sup>)<sup>17,36</sup> into the MSN was dependent to the solution concentrations of cytochrome *c*, which indicated that the encapsulation is a diffusion-driven process. As described in the Supporting Information, the amount of protein entrapped inside the MSN was determined by measuring the difference in concentration of cytochrome *c* in the supernatant before and after the loading of MSN. The maximum loading was determined to be 415.0 mg of cytochrome *c* per 1.0 g of MSN at the conditions studied. The XRD of a cytochrome *c*-encapsulated MSN with a loading of 95.0 mg/g MSN could still exhibit the hexagonal symmetry of the porous

structure with a lower contrast because of the pore-filling effect (Supporting Information Figure SI 4a). Also, the entrapment of cytochrome *c* inside the mesopores was observed in the nitrogen sorption analysis, where the BET surface area decreased from 1061 to 290 m<sup>2</sup>/g and the pore volume reduced from 1.82 to 0.19 cm<sup>3</sup>/g upon loading with cytochrome *c* at 95 mg/g (Supporting Information Figure SI 4b).

The release of cytochrome *c* from the MSN material at room temperature was studied by measuring the UV-vis absorption profile of the Soret band (412 nm) of cytochrome *c* in supernatant after separation of the solid MSNs by centrifuge. Two suspensions of cytochrome *c*-loaded MSN (100 µg/mL) were prepared in PBS buffer at two different pH values (7.4 and 5.2). These numbers were chosen to mimic the normal pH values in the cytoplasm and inside endosomes.<sup>37,38</sup> In both cases, a sigmoidal release curve was observed over a period of 25 h, which is characteristic of an energy-dependent release process. The total percent of loaded proteins that were released was 45% and 55% at pH 7.4 and 5.2, respectively (Figure 3). Given that the pI of cytochrome *c* is 10.5 and that the surface of MSN is rich in silanol groups ( $pK_a$  around 3), the protein is expected to be positively charged, whereas the MSN would be negatively charged at both pH values. Therefore, for cytochrome *c* molecules to be released from the mesopores, the favorable electrostatic interactions between the protein and the pore surface silicates need to be replaced by other ionic species in the solution similar to what has been observed in the literature.<sup>15,16,24</sup> The observed difference in the rates of release (Figure 3) at these two pH values could be attributed to the different amount of negative charges on the MSN surface. To test this hypothesis, we measured the change of the  $\zeta$ -potential of both MSN and cytochrome *c* as a function of pH (Supporting Information Figure SI 5). As expected, the  $\zeta$ -potential of the protein remained almost constant, with very little change (between +15 and +17 mV) between pH 5.5 and 8.0, whereas the  $\zeta$ -potential of MSN dropped dramatically from −25.5 mV at pH 7.35 to −1.81 mV at pH 5.22. This confirmed the surface charge property of MSN was indeed affected by the change in pH.

As shown in Figure 3, no significant release of cytochrome *c* from MSN was observed at pH 7.4 even after 4 h, while some release was observed immediately at pH 5.2. This difference in the rate of release of cytochrome *c* allows us to introduce the protein-loaded MSN to cell cultures under the physiological condition without losing a large amount of protein in the first 4 h. On the basis of the previous studies by us and others,<sup>32–34</sup> human cancer and other animal cells are able to internalize MSN materials within 1 h. The resulting endosome-entrapped protein–MSN material could then release cytochrome *c* molecules inside the cell.

To examine whether the MSN-released cytochrome *c* can still function as an active enzyme, we collected proteins that were released at pH 7.4 and tested the catalytic reactivity for the oxidation of 2,2'-azino-bis(3-ethylbenzthiazoline-6-sulfonate) (ABTS) by hydrogen peroxide. We compared the enzymatic activity of the MSN-released cytochrome *c* with that of the native protein at the same concentration and under the same conditions as described in the Supporting Information. As

(36) Berman, H. M.; Westbrook, J.; Feng, Z.; Gilliland, G.; Bhat, T. N.; Weissig, H.; Shindyalov, I. N.; Bourne, P. E. *Nucleic Acids Res.* **2000**, *28*, 235–242.

(37) Simoes, S.; Moreira, J. N.; Fonseca, C.; Duzgunes, N.; Pedrosa de Lima, M. C. *Adv. Drug Delivery Rev.* **2004**, *56*, 947–965.

(38) Tafani, M.; Cohn, J. A.; Karpnich, N. O.; Rothman, R. J.; Russo, M. A.; Farber, J. L. *J. Biol. Chem.* **2002**, *277*, 49569–49576.



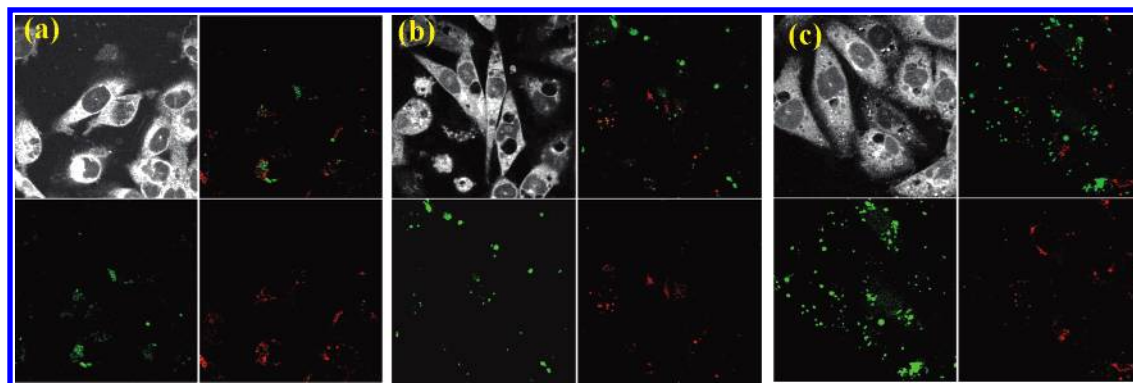


**Figure 6.** Uptake of FITC–cytochrome *c*-loaded MSN by HeLa cancer cells as observed by confocal fluorescence microscopy at the following incubation times: (a) 2, (b) 14, and (c) 24 h. For each set of pictures the upper left image is the autofluorescence image of the cells, the lower left corresponds to the green fluorescent protein taken up by the cells, the lower right shows the red fluorescent FM 4-64-labeled endosomes, and the upper right image is the merging of the green and red fluorescent images.

depicted in Figure 4, the kinetics of the two enzyme-catalyzed reactions are essentially identical, indicating that the MSN-released cytochrome *c* could serve as an active enzyme in aqueous solutions.

To exploit MSN as a transmembrane delivery carrier for intracellular controlled release of cytochrome *c*, we first covalently attached a fluorescent dye, fluorescein isothiocyanate (FITC), to the protein via a literature-reported procedure.<sup>39</sup> The labeling efficiency was determined to be 1.8 mol of FITC per mol of cytochrome *c* by UV–vis absorption spectroscopy. The fluorescein-labeled cytochrome *c* was then encapsulated inside the MSN by the aforementioned method described in the Supporting Information. The resulting cytochrome *c*-loaded MSNs were introduced to HeLa cell cultures with the cell density of  $1 \times 10^5$  cells/mL in D-10 growth medium. The uptake of the protein–MSN material by HeLa cancer cells was analyzed by flow cytometry. As shown in Figure 5, the flow cytometry result exhibited an efficient uptake with an  $EC_{50}$  of 33.6  $\mu\text{g/mL}$ . The cellular uptake of the material was also confirmed by confocal fluorescence microscopy. The uptake of MSN observed in this work is lower than the one we observed previously for MSN of smaller pore size ( $EC_{50}$  of 12.4  $\mu\text{g/mL}$ ).<sup>34</sup> This difference in uptake efficiency can be attributed mainly to the difference in particle size, for the smaller pore MSN has an average size around 150 nm, whereas the pore-enlarged MSNs are larger than that. It has been previously reported that an increase in the size of submicrometer particles usually leads to a decrease in the ability of cells to take them up.<sup>40</sup> To determine whether or not the cytochrome *c*-loaded MSNs could escape the endosomal entrapment, we stained the endosomes with a red fluorescent endosome marker (FM 4-64)<sup>41</sup> and monitored the confocal fluorescence micrographs (Figure 6) of FITC–cytochrome *c*-loaded MSNs in HeLa cells. The green fluorescent spots observed in Figure 6 represent the FITC–cytochrome *c*-loaded MSNs that were able to escape endosomes, whereas those that were entrapped inside of the vesicles exhibited yellow color, which is the result of overlapping red (endosome) and green (FITC–cytochrome *c*-loaded MSN) spots. As depicted in Figure 6a, there were a few FITC–cytochrome *c*-loaded MSNs trapped inside of endosomes within the first 2 h.

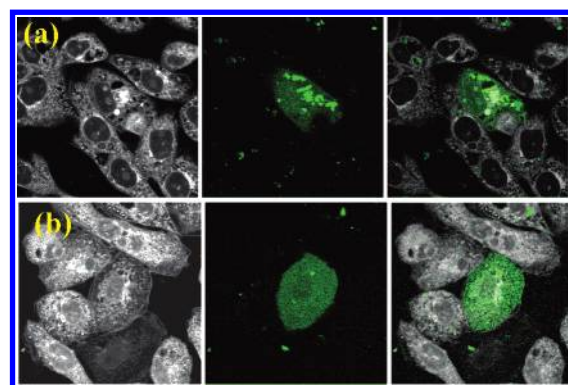


**Figure 7.** Confocal fluorescence images of HeLa cells displaying green fluorescence on their whole cell bodies, after incubation with FITC–cytochrome *c*-loaded MSN for (a) 18 and (b) 26 h. The left pictures correspond to the autofluorescence image of the cells when excited at 568 nm, the middle ones to the green fluorescent labeled protein (excitation at 488 nm), and the right ones to the merge of the first two.

However, as shown in Figure 6, parts b and c, no yellow spots could be observed in the micrographs indicating that there was no overlap between the green fluorescent FITC–cytochrome *c* and the red fluorescent endosomes. Our results clearly show that the FITC–cytochrome *c* could escape from the endosomes efficiently within a few hours of endocytosis. Interestingly, after 18 h of incubation, we observed an increasing number of HeLa cells displaying green fluorescence throughout their entire cell bodies (Figure 7) in addition to others that showed only isolated spots of green fluorescence inside the cytoplasm. Also, as depicted in Figure 7a, several spots with higher fluorescence intensities (FITC–cytochrome *c*-loaded MSN) could be observed inside the cell that displayed green fluorescence in the whole body. These spots faded away with time as the green fluorescence intensified throughout the whole cell body (Figure 7b). These results suggested that the fluorescein-labeled cytochrome *c* molecules were gradually released from the conglomerates of MSNs and were able to diffuse throughout the entire cytoplasm.

## Conclusion

In summary, we have demonstrated that the MSNs with large pores can host small membrane-impermeable proteins, such as cytochrome *c*, and release them under physiological conditions. Like the native cytochrome *c*, the protein released from MSNs

(39) Goding, J. W. *J. Immunol. Methods* **1976**, *13*, 215–226.

(40) Rejman, J.; Oberle, V.; Zuhorn, I. S.; Hoekstra, D. *Biochem. J.* **2004**, *377*, 159–169.

(41) Vida, T. A.; Emr, S. D. *J. Cell Biol.* **1995**, *128*, 779–792.

could also function as an active enzyme for oxidation reactions in aqueous solutions. These MSNs could serve as efficient transmembrane carriers to deliver cytochrome *c* into the cytoplasm of human cervical cancer cells (HeLa), while avoiding the endosomal entrapment. The intracellular release of the fluorescein-labeled cytochrome *c* was also observed by confocal fluorescence microscopy. Further development of these MSN-based controlled release systems for protein delivery may lead to breakthroughs for many therapeutics and metabolic manipulation applications.

**Acknowledgment.** The authors are thankful for the financial support for this research from the U.S. National Science Foundation (CHE-0239570) and from the U.S. DOE Ames Laboratory through the office of Basic Energy Sciences under Contract No. DE-AC02-07CH11358.

**Supporting Information Available:** TEM and SEM images, nitrogen sorption analysis, XRD patterns, and size distribution of the large-pore MSN, variation of  $\zeta$ -potential with pH, and the Experimental Section. This material is available free of charge via the Internet at <http://pubs.acs.org>.

JA0719780